12 Mar 1991, 10:30 am - 12:00 pm

General Report Session 4: Dynamic Earth Pressures and Seismic Design of Earth Retaining Structures

R. Richards Jr.

State University of New York at Buffalo, New York

Proceedings: Second International Conference on Recent Advances in Geotechnical Earthquake Engineering and Soil Dynamics, March 11-15, 1991 St. Louis, Missouri, General Report No. IV

Dynamic Earth Pressures and Seismic Design of Earth Retaining Structures

R. Richards, Jr.
USA

INTRODUCTION

The great number of significant variables which effect the seismic behavior of retaining structures make this both a fascinating subject and a difficult one. The ten papers in this session cover both elastic and plastic aspects of analysis and design for a wide variety of wall types. To help put them in perspective, a new, fundamental seismic free-field solution will be reviewed briefly. This will serve as a benchmark from which the effects of changing the lateral boundary condition by introducing various types of walls can then be evaluated.

INERTIAL ELASTIC-PLASTIC FREE FIELD

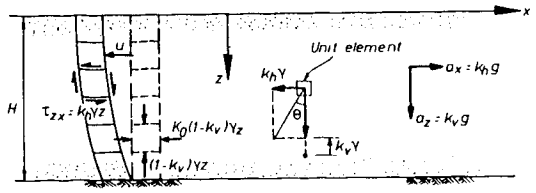

Fig 1. Seismic Free Field

When uniform horizontal and vertical acceleration components are applied to a homogeneous horizontal layer of granular soil of infinite lateral extent with unit weight γ (Fig. 1), the two-dimensional differential equations of equilibrium become:

$$\frac{\partial\sigma_x}{\partial x}+\frac{\partial\tau_{xz}}{\partial z} = k_h\gamma \qquad (1)$$

$$\frac{\partial\tau_{xz}}{\partial x} + \frac{\partial\sigma_z}{\partial z} = (1-k_v)\gamma$$

with the solution

$$\sigma_x = K(1-k_v)\gamma z$$

$$\sigma_z = (1-k_v)\gamma z \qquad (2)$$

$$\tau_{xz} = -k_h\gamma z$$

Essentially, this dynamic solution for the free field is the static free-field solution with a unit weight of $(1-k_v)\gamma$ superimposed with a pure-shear field introduced by the horizontal acceleration. The stress/strain relationship is assumed to be linear (*with* $\epsilon_z = 0$) and the deformation due to the shear:

$$u = -k_h\frac{\gamma(H^2-z^2)}{2G} \qquad (3)$$

in terms of the shear modulus G, is parabolic as shown in Fig. 1.

This free-field solution requires that either the lateral boundary force and displacement be distributed exactly as the solution dictates or by St. Venant's principle, we are "far enough away" from the lateral boundaries.

As shown in Fig. 2, k_v has no direct effect on the factor of safety against yield but simply moves the Mohr's Circle back and forth within the K_o line.

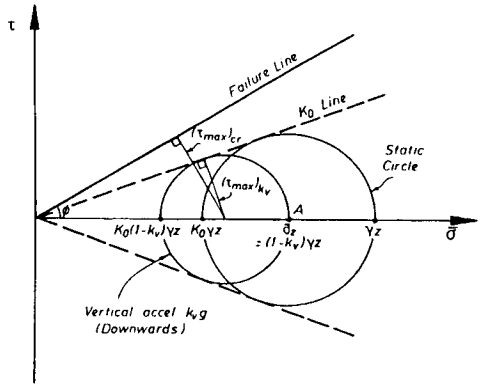

Fig. 2. Effect of Vertical Acceleration: $a_z = k_v g$

Rather, it is the horizontal acceleration component that directly drives the stress state toward the failure line by introducing shear. Only indirectly may k_v participate by changing the absolute amount which k_h must increase τ_{max} to reach its limit. Further k_h, unlike k_v, rotates the principal axes in the process. This is shown in Fig. 3, where the initial stress on a horizontal surface before application of horizontal acceleration is at point A on the σ-axis, with a value of $\sigma_z = (1-k_v)\gamma z$.

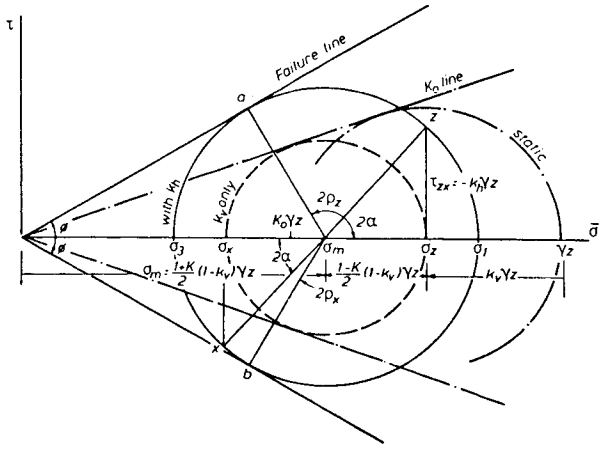

Fig. 3: Initial Yield (Fluidization)

This is the same as point A in Fig. 2. Addition of an increasing horizontal acceleration will produce a shear stress component, $\tau_{zx} = -k_h \gamma z$ which will move the stress point along a stress path vertically upward (or downward, depending on the sign). The Mohr circle will increase in diameter about a fixed center until, at a stress represented by a or b, the Mohr circle touches the failure lines and shear flow can take place. It has been assumed that ϕ remains constant even though in practice it might vary with location and deformation. A constant value is justified in a limit analysis using either peak or residual values.

This state of potential shear flow is called initial fluidization by Richards, Elms and Budhu (1990). If Jaky's simplified expression, $K_o = 1-\sin\phi$, is assumed, the associated acceleration components and slip surfaces can be computed directly.

Another solution is possible. A Mohr circle could be drawn through point z, touching the yield lines but with its center to the right of A. This is the passive case and would give a value of K considerably greater than unity. As will be seen later, with increasing lateral acceleration levels the active and passive conditions will approach each other and ultimately converge.

The counterclockwise orientations of the slip surfaces ρ_z and ρ_x are most easily referred to the major and minor principal planes by the following formulas:

$$\rho_z = 45 + \frac{\phi}{2} - \alpha \qquad (4)$$

$$\rho_x = 45 - \frac{\phi}{2} - \alpha = \rho_z - \phi$$

where the angle, α, by which the principal planes are rotated clockwise due to k_h is given by

$$\tan 2\alpha = \left(\frac{k_h}{1-k_v}\right)\frac{2}{1-K} = \tan\theta\,\frac{2}{1-K} \qquad (5)$$

When the horizontal acceleration reverses, so does the direction of the shear and therefore the directions of α, ρ_z, and ρ_x. It is important to note that γ and z have canceled, so, as in the static case (for no wall friction), slip surfaces are straight and extend through the depth of the layer.

From the geometry of Fig. 3, the Mohr-Coulomb failure criterion can be expressed as

$$\left[\frac{1+K}{2}(1-k_v)\gamma z\right]\sin\phi = \left\{\left[\frac{(1-K)}{2}(1-k_v)\gamma z\right]^2 + (k_h\gamma z)^2\right\}^{1/2} \qquad (6)$$

Then

$$\left(\frac{k_h}{1-k_v}\right)^2 = \tan^2\theta = K - \left(\frac{1+K}{2}\right)^2\cos^2\phi \qquad (7)$$

Solving for K gives

$$K = \frac{1+\sin^2\phi}{\cos^2\phi} \pm \frac{2}{\cos\phi}\left(\tan^2\phi - \tan^2\theta\right)^{1/2} \qquad (8)$$

In the free field, shear flow does not occur and accelerations greater than those which would cause initial fluidization can be tolerated. Now as accelerations increase the lateral pressure σ_x increases in the active case and decreases in the passive case and the limiting Mohr's circle for each case move toward each other until the slip surfaces, both active and passive, become horizontal and the two cases converge. At this ultimate state called general fluidization:

$$(\tan\theta)_F = \left(\frac{k_h}{1-k_v}\right)_F = \tan\phi \qquad (9)$$

corresponding to

$$K_{EF} = \frac{1+\sin^2\phi}{\cos^2\phi} = \frac{K_A+K_P}{2} \qquad (10)$$

At this point the soil can not transmit further acceleration and the soil acts very much like a viscous fluid.

Thus equations 4-8 derived by Richards et al (1990) describe with Mohr's circle the full-range, elastic-plastic dynamic behavior of the semi-infinite layer of an ideal elastic-plastic soil at all stages of inertial loading.

In one sense they are the dynamic counterpart to Coulombs'static equations for the Rankine limit state published in 1776 just as the Mononobe-Okabe equations are the dynamic-counterpart to Coulombs' static minimization of an assumed sliding-wedge failure mechanism used for more general geometry and assumed wall friction. However these dynamic equations are much more powerful than the M-O equations in that they give a full-field solution showing how the normal and shearing stresses build up with increasing earthquake intensity until, at $\theta = \phi$, the shear wave can no longer be transmitted.

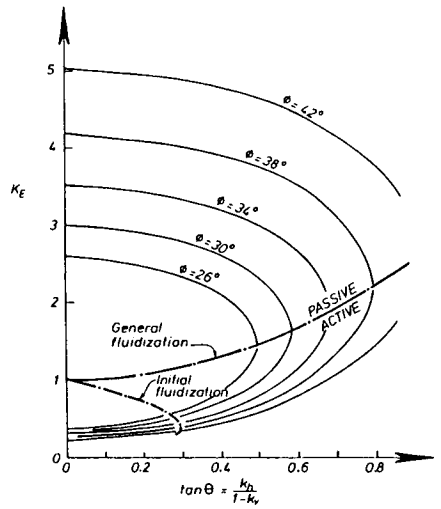

Fig. 4: Coefficient of lateral Pressure - Free Field

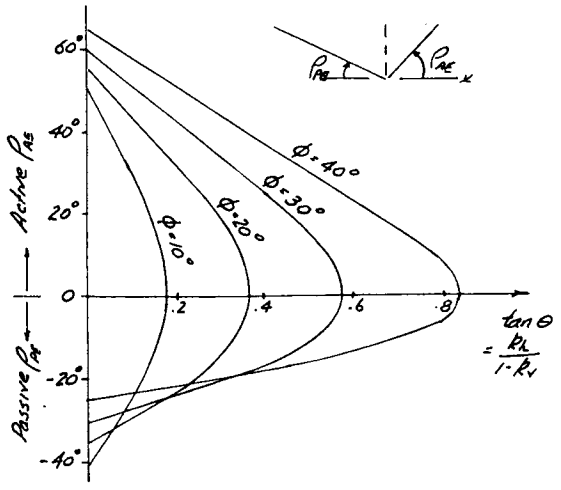

Fig. 5: Inclination of the Critical Surface - Free Field

The various stages of seismic fluidization as a function of ϕ and acceleration intensity are shown in Fig's 4 and 5. Until initial fluidization there is no seismic increase in lateral pressure due to horizontal acceleration since only shear is introduced and vertical sections deform parabolically (Eq'n 3). Above this acceleration intensity lateral pressures develop allowing greater shear stresses to develop and rotating the potential slip surfaces toward the horizontal. The initial fluidization state

for ϕ = 30° is shown in Fig. 6. In Fig. 7 two free body diagrams are plotted to illustrate the equations.

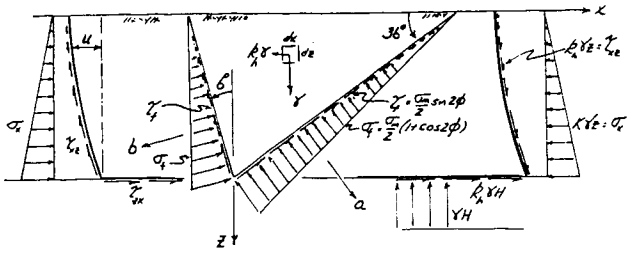

Fig. 6: Critical Stresses

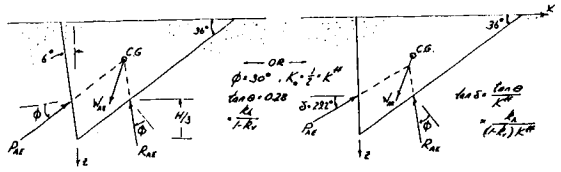

Fig. 7: Equilibrium at Initial Fluidization

For the vertical plane the free field solution shows that the angle of friction, δ, is given by the expression

$$\tan \delta = \frac{\tan \theta}{K} \qquad (11)$$

where K for the free field has already been defined as the ratio of horizontal to vertical stress.

The M-O equations based only on force analysis will give identical results only if the correct angle of friction, given by Eqn. 11, is used.

SEISMIC BEHAVIOR OF RETAINING WALLS

The free-field solution will give the correct stresses on a retaining wall if it deforms exactly as dictated by the free-field thereby maintaining the correct interface boundary condition. However, it is unlikely that any wall can be designed to do this even though it would be optimum in the structural sense that the soil would not "know" the wall existed. Real walls therefore violate the interface boundary condition changing the contact stress distribution by enforcing displacements other than free-field.

Rigid, Nonsliding Walls

Two papers deal with the extreme case of a rigid, nonsliding wall, such as some basement walls, channel linings or abutments. SOYDEMIR (paper no. 6) reviews previous work on this case which shows that the dynamic increment is much higher in magnitude and position than the M-O distribution. ORTIGOSA & MUSANTE (paper no. 8) make the same observation. Figure 8 from their paper compares the dynamic increment of pressure σ_x for various elastic methods of analysis. Ortegosa and Musante also consider a perhaps more realistic nonlinear case where the shear modulus increases with the square root of the depth.

The concept for this "elastic" approach is straightforward. The rigid wall must completely eliminate the free-field displacement (Eqn'. 3). This correction can be computed to various degrees of sophistication (Fig. 8) including the "kinematic method" outlined in paper #8. Essentially this is a shear transfer situation and Fig. 9 computed by this reporter by both finite-element and boundary element methods shows how the rigid wall effect dies off into the free-field.

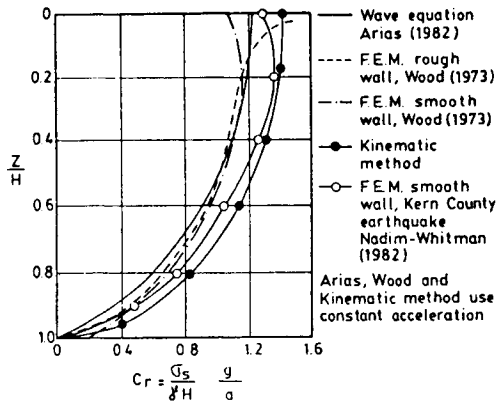

Fig. 8: Seismic Pressure on a Rigid Wall (Paper #8)

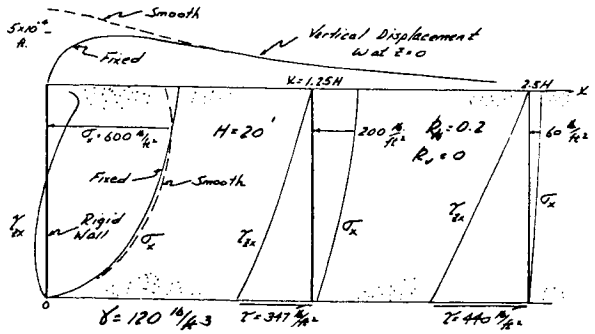

Fig. 9: Seismic Pressure Increment with a Rigid Wall

As pointed out in both papers, it is very important that for rigid, immobile walls, these results should be recognized in design. Geotechnical engineers study these excellent papers in detail. The analysis is simple and if the computed dynamic "correction" increment for the rigid wall is added to the free-field distribution the resulting seismic design will be satisfactory.

Flexible-Nonsliding Walls

Real walls are flexible to some extent or they may be purposely designed to develop plastic hinge lines in severe earthquakes. Any movement of the wall will reduce the seismic pressures from the maximum rigid distribution toward the minimum free-field. Any number of possibilities can be considered. For free-standing walls, the case considered by Ishibashi and Fang discussed in Soydemir's paper is the classic situation where a hinge develops at the base of a non-sliding wall. A rotation at the base of only 5 x 10^{-4} radians is sufficient to reduce the lateral pressure distribution to nearly that of the free-field.

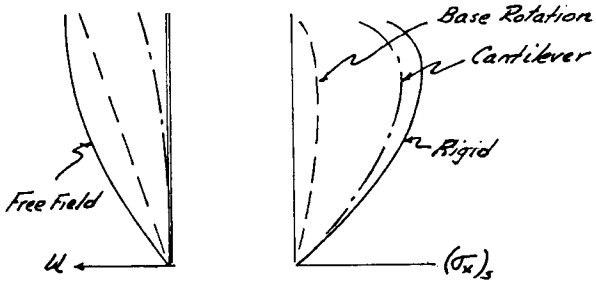

Fig. 10: Dynamic Increment for "Elastic" Wall Movements

Considering the wall as a cantilever beam of a given stiffness, the deformation is much less like the free field and Ortigosa and Musante show that, as might be expected, the attenuation of lateral stresses is less and the distribution is more like the rigid case (Fig. 10).

Earth-Reinforced walls discussed by FONDASOL and KNOCHEN-MUS (paper #5) have the potential to approach the free field condition. In their paper they review the various empirical methods for analysis and design where the reinforced earth is considered as an equivalent wall with its own inertial contribution. However, from their presentation and work by others (reviewed by Elms & Richards, 1990) it appears that, if properly designed, reinforced earth walls can behave as ideal shear beams minimizing lateral pressures. More comprehensive finite-element dynamic analysis of reinforced earth leading to such designs would seem to be a fruitful area for future research.

Walls with Sliding

Walls that are not laterally braced will slide at their base even in moderate earthquakes (Richards & Elms, 1979). When this occurs an elastic-type solution, while it can give some physical insight, will not be accurate since plastic shear flow takes place with subsequent redistribution of the stress field. Since the displacement field is discontinuous the stress field must be nonlinear and the complexity of the description of seismic behavior increases by at least an order of magnitude.

Two approaches to analysis and design can be followed to approximate this difficult limit-analysis problem: The first is to use a lower-bound type, finite element model incorporating non-linear and yield properties of the soil with or without pore-pressure strength degradation coupled with slip elements, springs and dashpots at the boundaries all formulated to various degrees of sophistication. The paper by ALAMPALLI and ELGAMAL (paper #10) gives a good review of work on this approach and presents a state-of-the-art finite-element model which accounts for wall and soil resonance, nonlinear wall-backfill soil interaction, simultaneous base sliding and rotation, non-linear soil properties, and possible pore pressure buildup. Although not related to either field or laboratory observations for verification, interesting results are presented for a 15 m high cantilever wall, which demonstrate the power of this approach and the potential with increasing computational power to better understand the seismic behavior of all types of walls at a global scale.

Certainly some such model would be necessary, for example, to explain the behavior of the fiber-reinforced sand wall reported by FUKUOKA AND OKEDOI (paper #12). The behavior of this structure carefully documented during construction under static conditions and also subjected to moderate earthquake, is unusual and presents an excellent example to use to verify advanced finite-element models. Such walls, backfilled with cohesive material are more like reinforced slopes and fall into no normal category. The highly nonlinear reinforced sand yields internally and deforms plactically during construction so that even a standard static computation overestimates the active earth pressure by 300%. The seismic increase at $k_h = 0.1$ is better with the M-O analysis exceeding the recorded value by only 10% to 60%

The second approach to seismic analysis and design of retaining walls with base sliding and/or significant rotation is upper-bound limit analysis. The simplest solution is obtained by assuming classic Coulomb failure wedges with inertia to calculate the force on the wall (given by the M-O equations for regular geometry) combined with a Newmark sliding-block model, including the inertia of the wall itself when necessary, to calculate displacements. Because this strategy is so straightforward, intuitively satisfying, easy, and powerful for making design decisions it has received the most attention since its introduction Richards and Elms, 1979) and many refinements have been suggested (see Whitman,1990; Elms and Richards, 1990 for recent reviews and further references).

One open question is the position of the resultant force, P_E, delivered to the retaining wall from the seismic sliding wedge. Although it is often stated in the literature that the M-O equations predict the resultant at the third point (a hydrostatic distribution of pressure) this is not true. As the free-field equations demonstrate, a hydrostatic distribution only occurs if the wall does not slide and deforms parabolically (Eqn. 3) The M-O equations or the more general Coulomb sliding-wedge limit analysis is based entirely on force equilibrium since, even with an assumed δ, the moment equilibrium equation for the wedge is indeterminate. Thus, while the magnitude of the seismic thrust, P_E, on walls which move enough to develop a "failure" mechanism may be determined with good accuracy from equilibrium, the distribution of contact stresses and therefore the position of the resultant thrust depends on the deformation of the wall.

As was done in the "elastic" range of small deformations, a basic understanding of what distribution of P_E should be expected for each basic type of wall movement in the plastic range is possible by comparison to the free-field solution which is valid at all acceleration levels. Since no tension is possible, the plastic redistribution of lateral pressure observed experimentally and shown in Fig. 11 is perfectly understandable. In zones where seismic displacements exceed the free field and there would be "elastic" tension, pressures are reduced from the hydrostatic value to build up in areas where there is still excess compression compared to the free field distribution.

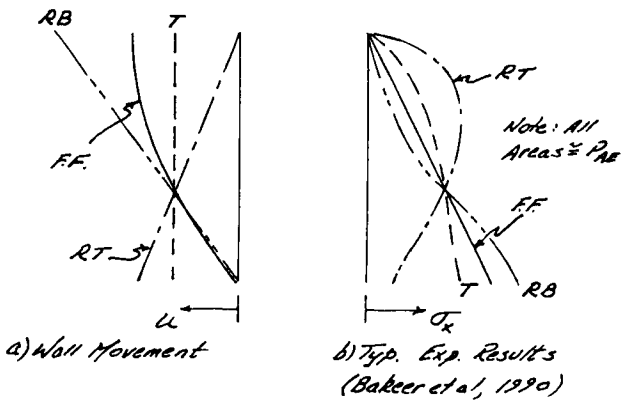

Fig. 11: Plastic Stress Distributions with Various Wall Movements

However, to derive a sample analytic method to capture this redistribution is more difficult. The paper by DEWAIKAR (paper #22) attempts to do this by using the method of slices for the critical Coulomb wedge with a unknown variation of friction angle between slices chosen so as to maximize the overturning moment. The concept is interesting and deserves more investigation. As formulated now there is no differentiation as to the type or amount of wall movement and both experimental results (Bakeer et al, 1990) and our previous discussion would indicate that the height of P_{AE} would be relatively independent of acccleration intensity.

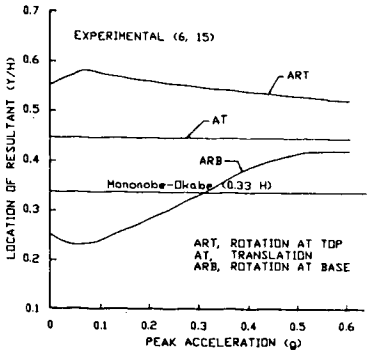

Figure 12. Experimental Location of the Resultant (Bakeer et al, 1990)

A different analytic approach is proposed by ELMS and RICHARDS (paper #9) where Dubrova's method to determine the height of the static thrust is extended to the seismic case. The results show the effect expected (Fig. 11) for each type of wall movement but not to the extent measured experimentally (Fig. 12). This may be due to a possible peak vs. residual strength effect discussed paper #9 which also raises the center of pressure and increases with large wall movements at higher accelerations.

Certainly the location of the thrust, either active or passive, is important for design where rotation as well as sliding is possible. A relatively simple method for computing coupled rotation and sliding of a rigid gravity wall by a Newmark-block incremental model is presented by SIDDHARTHAN AND GOWDA (paper #15). Compression of the foundation is modeled by springs and both the center of rotation and position of P_{AE} are unknown. An interesting parametric study shows that under certain conditions tilting is possible leading to large incremental movement at the top of the wall. This emphasizes the importance in seismic designs of selecting a wall geometry to avoid this possibility. Tests and field observations of gravity walls indicate that, in fact, rotation of most walls designed statically slide before they rotate but further experimental work to better define this case and verify mixed-mode, limit-analysis models such as proposed in paper #15 would be worthwhile.

Tied-Back Walls

An even more difficult, mixed-mode, situation occurs with quaywalls, anchored bulkheads or other types of tied-back retaining structures. While the majority of earthquake failures of such structures result from liquification, many are due to increased active pressures and decreased passive resistance at both the base and the anchor. These effects which can combine in various ways are shown in Fig. 13. Both the failure of a particular quaywall at Akita Port in the 1983 Nihonkai Chubu 7.7 magnitude earthquake analyzed by IAI AND KEMEOKA (paper #14) and the survey by Kitajima and Uwabe of 110 bulkheads in Japan reviewed by GAZETAS and DAKOUOAS (paper #23) indicate, when liquification does not predominate, it is usually the anchor which is the weak seismic component in current designs.

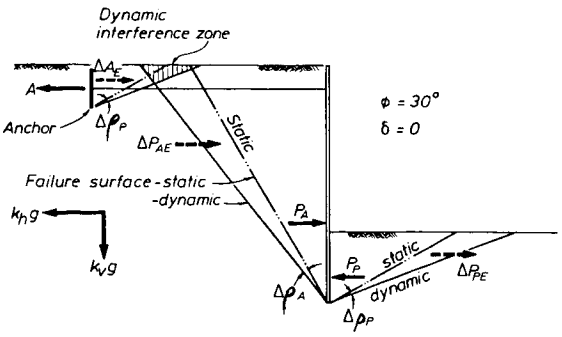

Fig. 13: Seismic Effects on Tied-Back Walls

Three effects are involved. Initially the anchor makes the top part of the wall more rigid building up seismic pressures on the wall well above the free-field value greatly increasing the anchor force. At the same time the resistance available to take the pull is decreased because of the inertial contribution in the passive case. Finally, and perhaps most important, the active wedge grows in size by $\Delta\rho_A$ interfering with the passive anchor wedge further reducing the seismic anchor capacity. Thus the anchor lurches outward at each excursion of acceleration above the critical level triggering outward movement of the top of the wall accompanied by cracking and settlement behind the anchor. This typical failure mode is illustrated in paper #23, and reproduced in Fig. 14. It is also similar to that reported by Iai and Tomohiro for Ohama no. 2 Wharf which they analyzed in detail with a combined finite element and spring model which includes pore-pressure buildup with cyclic degradation of strength.

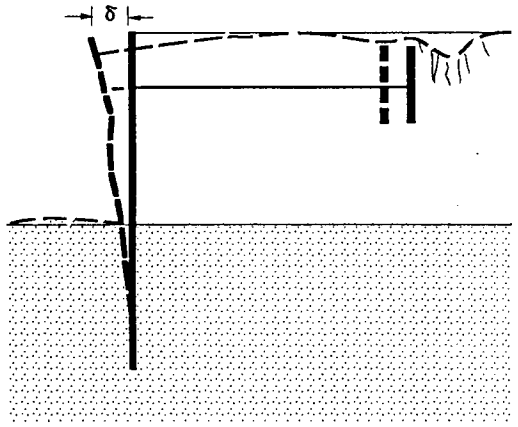

Fig. 14: Typical Seismic Deformation of a Statically-Designed, Tied-back Wall (paper #23)

Clearly tied back walls are a productive area for future study using both using both lower-bound and upper bound strategies. Gazetas and Dakoulas convincingly show that the current Japanese seismic code is deficient and illogical and suggest how it might be modified to strengthen the anchor. This, in turn, could lead to passive failure at the toe. This failure mode involving rotation about the top has been demonstrated in centrifuge tests (Steidman and Zeng, 1990) and is also observed occasionally in the field. A balanced design philosophy where anchor and toe movement occur simultaneously with translation of the wall at the critical design acceleration would seem to be a logical basis for future codes (as it is now for structural concrete).

SUMMARY

This report in no way does justice to the papers submitted to this session. All ten papers are interesting and worthwhile sheding light on various aspects of this broad area of "seismic earth pressures and the analysis and design of retaining structures". Rather this report is designed to initiate discussion by concentrating on the fundamental idea of suggesting how various wall types can perturb the first mode of the seismic free field which ideally exists before construction.

Ten years ago at the time of the first conference this subject was really in its infancy. Today it is perhaps an adolescent. Certainly we have a much better understanding and a clearer seismic design procedure for walls of all types. Twenty topics could easily be listed where significant research is needed to nurture further growth. Better analytic and experimental models, for example, should lead to a much clearer picture of dynamic soil-water interaction so crucial in the behavior of so many real walls and now disregarded or only poorly estimated for most designs. However, this impulse to enumerate potential for areas of future study is resisted since ingenuity, enthusiasm, and insight seldom evolves from a research shopping list. Moreover, judging from the questions raised by these excellent papers, such a list is not necessary and we can look forward to a session in 2001 when our understanding of seismic pressures and the behavior of retaining structures will have reached maturity.

REFERENCES

Bakeer, R.M., Bhatia, S.K., and Ishibashi, I. (1990) "Dynamic Earth Pressure with Various Gravity Wall Movements"; Design and Performance of Earth Retaining Structures Geotec. Special Pub. No. 25, ASCE, pp. 887-899.

Elms, D.G. and Richards, R., Jr. (1990) "Dynamic Earth Pressure with Various Gravity Wall Movements"; Design and Performance of Earth Retaining Structures Geotec. Special Pub. No. 25, ASCE, pp. 854-871.

Richards, R. Jr., Elms, D.G. and Budhu, M. (1990) "Dynamic Fluidization of Soils", Jour. of Geotech. Eng'g, Vol 116, No. 5, ASCE pp. 740-759.

Richards R. Jr. and Elms, D.G. (1979) "Seismic Behavior of Gravity Retaining Walls", Jour. of the Geotech. Eng'g Div., Proc. ASCE, Vol. 105, No. GT4, pp. 449-464.

Steedman, R.S. and Zeng, X. (1990) "Dynamic Earth Pressure with Various Gravity Wall Movements"; Design and Performance of Earth Retaining Structures Geotec. Special Pub. No. 25, ASCE, pp. 872-886.

Whitman, R.V. (1990) "Dynamic Earth Pressure with Various Gravity Wall Movements"; Design and Performance of Earth Retaining Structures Geotec. Special Pub. No. 25, ASCE, pp. 817-842.